01 Jun 2022

A Planar Low-Profile Meander Antenna Design for Wireless Terminal Achieving Low RF Interference and High Isolation in Multi-Antenna Systems

Yang Xiao

Yihong Qi

Wei Yu

Ye Hai Bi

et. al. For a complete list of authors, see https://scholarsmine.mst.edu/ele_comeng_facwork/4647

Recommended Citation

Y. Xiao et al., "A Planar Low-Profile Meander Antenna Design for Wireless Terminal Achieving Low RF Interference and High Isolation in Multi-Antenna Systems," *IEEE Transactions on Electromagnetic Compatibility*, vol. 64, no. 3, pp. 674 - 682, Institute of Electrical and Electronics Engineers, Jun 2022.
The definitive version is available at https://doi.org/10.1109/TEMC.2021.3133569

A Planar Low-Profile Meander Antenna Design for Wireless Terminal Achieving Low RF Interference and High Isolation in Multi-Antenna Systems

Yang Xiao, *Student Member, IEEE*, Yihong Qi, *Senior Member, IEEE*, Wei Yu, *Member, IEEE*, Ye-Hai Bi, Xiangrui Su, *Student Member, IEEE*, Chunyu Wu, Qiang Liu, *Member, IEEE*, and Jun Fan, *Fellow, IEEE*

***Abstract*—In this article, a meander line internal antenna used for wireless terminal is proposed. The current of this antenna is mostly distributed on the antenna radiator itself, rather than on the main board of the wireless device. As a result, the chance of having radio-frequency (RF) interference issues, which usually result in receiver desensitization in wireless radios, can be significantly reduced. The antenna has good radiation performance in the vertical polarization with a low physical profile, compared with the existing antenna designs for typical wireless terminals. The antenna has efficiency similar to the monopole antenna with much less reference/ground plane dependence, achieving lower RF interference, which is demonstrated by the noise coupling measurements in a predefined digital clock - antenna configuration. Furthermore, the mutual coupling (i.e., isolation) between two such antennas is studied and the envelope correlation coefficient between the two antennas is found to be low. A router assembled with the two proposed antennas is tested, and the total isotropic sensitivity is found lower compared with monopole antennas, due to the characteristics of low RF interference and high isolation of the proposed antenna.**

***Index Terms*—Envelop correlation coefficient (ECC), isolation, low profile, planar meander antenna, receiver desensitization, reference/ground plane dependence, radio-frequency (RF) interference, vertical polarization, wireless terminal.**

I. Introduction

Wireless access point (AP) terminals or wireless routers are widely used in both consumer and industrial applications for wireless internet connections and other wireless services. The AP antenna performance is a critical parameter to determine the coverage of these wireless terminals in a multipath environment. Wireless terminal radio signal coverage is dependent on antenna polarization, antenna efficiency, radio receiver sensitivity, etc. The commodity nature of the AP terminals also makes the AP antenna price sensitive.

In indoor communication environments, around half of the electrical energy is in the vertically polarized wave [1], [2]. Hence, any antenna having high vertical polarization generally has better coverage in indoor communication environments. External dipole and monopole antennas are the most commonly used AP antennas in commercial products. External monopole antennas have the advantages of high antenna efficiency and high vertical polarization. However, these antennas are large in size and usually use expensive radio-frequency (RF) connectors for connection.

Antenna size can have a large impact on wireless terminal ergonomic design, as well as wireless terminal installation (since some terminals are placed against walls or under tables or cabinet). In addition, the wireless terminal itself is getting smaller and slimmer. Therefore, internal low-profile antennas, such as the printed monopole and the inverted-F antenna, are becoming more popular [3]–[9]. Both of these antennas are reference plane dependent, increasing their susceptibility to RF interference. In most radio receivers, the antenna reference planes are the ground planes of the RF and digital circuits. One significant issue with the ground plane as a part of the antenna is RF interference. High-speed digital circuits can cause a large noise current to flow on the ground plane of a printed circuit board (PCB). This noise current can be easily coupled to the antenna, resulting in RF interference issues, if the ground plane is part of the RF antenna. Receiver desensitization is the main consequence of RF interference from the digital part of the device to the RF radios, which degrades the throughput of the radio receiver.

Multiple input and multiple output (MIMO) is commonly used to improve system communication data rate in a multipath environment. In order to enhance receiving capability and throughput, multiple AP antennas are placed in an AP terminal. Isolation in terms of the envelope correlation coefficient (ECC) among the antennas should be taken into consideration. A low ECC is one of the key factors for achieving better throughput of the radio receiver.

Manuscript received May 26, 2021; revised October 27, 2021; accepted November 19, 2021. Date of publication January 13, 2022; date of current version June 13, 2022. This work was supported in part by Natural Science Foundation of Hunan Province of China under Grant 2021JJ30143, and in part by Changsha Municipal Natural Science Foundation under Grant kq2007034. *(Corresponding author: Qiang Liu.)*

Yang Xiao and Qiang Liu are with the School of Electrical and Information Engineering, Hunan University, Changsha 410082, China (e-mail: xiaoyang1@hnu.edu.cn; lqxx1982@gmail.com).

Yihong Qi is with Peng Cheng Laboratory, Shenzhen 518000, China, and with the , also with Link-E Technology (Hengqin) Co., Ltd., Zhuhai 519070, China, and also with School of Electrical and Information Engineering, Hunan University, Changsha 410082, China (e-mail: qiyh@pcl.ac.cn).

Wei Yu is with General Test Systems Inc., Shenzhen 518055, China (e-mail: fred.yu@generaltest.com).

Ye-Hai Bi is with the Shenzhen Sunway Communication Company, Ltd., Shenzhen 518104, China (e-mail: yehai_bi@126.com).

Xiangrui Su, Chunyu Wu, and Jun Fan are with the EMC Laboratory, Missouri University of Science and Technology, Rolla, MO 65409 USA (e-mail: suxia@mst.edu; cw967@mst.edu; jfan@mst.edu).

Color versions of one or more figures in this article are available at https://doi.org/10.1109/TEMC.2021.3133569.

Digital Object Identifier 10.1109/TEMC.2021.3133569

In this article, a novel planar, low-profile, high-efficiency antenna, denoted planar low-profile meander antenna (PLMA) is presented. Compared with the classic monopole antennas, it not only has comparable antenna efficiency and vertical antenna gain, but also has less current distributed on the ground plane of the main PCB. This makes it less ground-plane dependent. Therefore, less RF interference issues are expected in the wireless terminal using the proposed antenna, which can result in higher throughput. Two prototypes of the PLMA antennas working at 2.4 GHz were fabricated to validate the designs, and the measured results show better ECC performance and lower RF interference than monopole antennas. Furthermore, the proposed antenna has low profile, and is easier to be incorporated in a variety of router designs. The proposed antenna designs are presented in Section II, together with the simulation and measurement results. In Section III, the proposed PLMA is compared with the conventional λ/4 monopole antenna, and an experiment on studying its noise coupling characteristics compared with the monopole is conducted. In Section IV, isolation between two proposed PLMA antennas (in terms of ECC) is compared with that of the λ/4 monopole antennas. Meanwhile, PLMAs are assembled in a router and the receiver sensitivity of the router is tested. Finally, the conclusion is presented in Section V.

II. Single Low-Profile Meander Antenna Design

A. *Design Concept*

In general, the common impedance coupling could be the dominating noise coupling mechanism, in which the antenna shares the reference plane with the RF circuit. Therefore, an antenna that has less current distributed on the reference plane has less chance of coupling noise. For the conventional λ/4 internal monopole antenna, it's equivalent to an asymmetric dipole antenna: the monopole is the short arm, whereas the reference plane becomes the long arm. Naturally, the monopole has a feature of wideband with a larger area of reference plane, the currents are spread over the reference plane, which increases the chance of noise coupling.

The proposed PLMA is based on a traditional full wave (1λ) wire antenna, Fig. 1(a) shows a full-wave antenna and the current flowing on it. There are two current antinodes on the wire, the currents near two antinodes are the main radiation sources. The antenna is folded such that the two sections with the strong current are in the vertical direction and the phase of the current flowing in these two sections are the same. In order to get a more compact size, some parts of the wire antenna are designed as a meander line, which is a typical method for compact size design especially for low-frequency antennas, such as RFID antennas [10]–[12]. The meander design could reduce the antenna physical size, and more importantly, the meander design is placed at specific locations having relatively smaller antenna current; thus, the effects of the meander design on antenna performance are minimized.

As illustrated in Fig. 1(b), the two sections with larger antenna current are kept as straight lines. Then, the meander line is introduced as shown in Fig. 1(c). The feeding point is placed at one end of the folded wire. This specific design aims to enhance antenna efficiency and vertical antenna gain, and at the same time decrease antenna height. With the help of higher quality factor of the full-wave antenna, the ratio of maximum current density between radiator and reference plane of the proposed antenna is higher than a conventional quarter-wavelength monopole. Since the RF currents are mainly distributed on the proposed antenna itself, therefore, chances of coupling noise will be reduced. It should also be noted that if the antenna is all fabricated on the FR4 material, more energy will be dissipated in this lossy substrate. The antenna vertical polarization gain is also proportional to the vertical antenna size and current distribution.

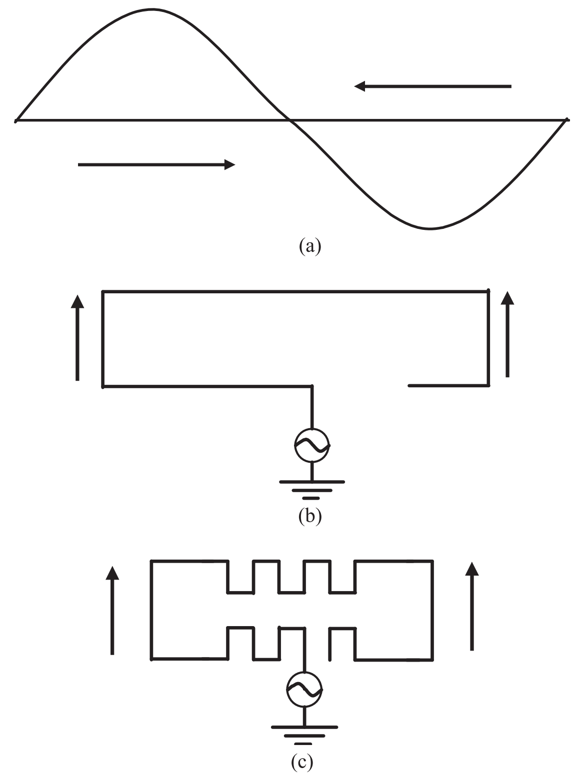

Fig. 1. Design concept of low-profile meander antenna. (a) Traditional full-wave wire and its current distribution. (b) Folded antenna. (c) Wire antenna with meander line design.

B. *Proposed 2.4-GHz PLMA*

A 2.4-GHz PLMA was designed and fabricated with its geometry illustrated in Fig. 2(a). The antenna was etched on an FR4 substrate with a thickness of 0.8 mm, a dielectric constant of $\varepsilon_r = 4.4$, and loss tangent of $\tan\delta = 0.027$. Then, the antenna board was placed close to the center of one side of a 10 cm × 10 cm main PCB for testing. The antenna was fed by a coaxial cable RG-405. The center pin of the coaxial cable was soldered to the antenna, whereas the outer conductor was soldered to the ground plane of the main PCB. The detailed antenna structure is shown in Fig. 2(b), and the feeding portion is illustrated in Fig. 2(c).

The dimensional parameters shown in Fig. 2(b) and (c) are L1 = 35, L2 = 22, L3 = 5, W1 = 1, W2 = 1, W3 = 0.5, S1 = 7, S2 = 6.5, H1 = 19, H2 = 4, H3 = 11, and H4 = 4 mm.

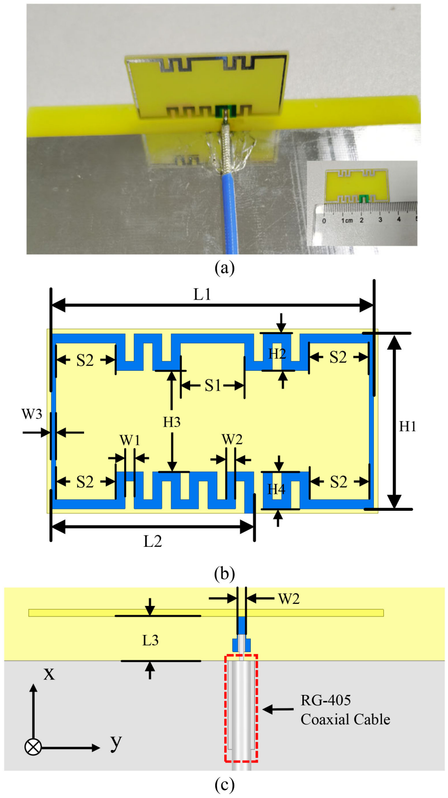

Fig. 2. Geometry of the proposed 2.4-GHz PLMA. (a) Antenna placed close to the center of the PCB. (b) Detailed meander line structure. (c) Position of antenna feeding port.

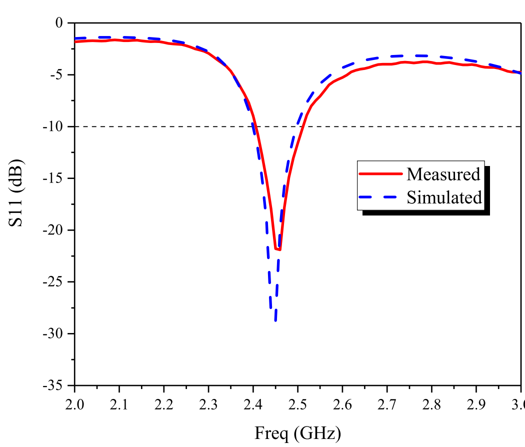

Fig. 3. Measured and simulated S-parameter plot of the proposed 2.4-GHz PLMA.

The antenna geometry shown in Fig. 2 is simulated using Ansys HFSS. The antenna height is set as 19 mm to achieve a relatively strong vertical polarized component while keeping the low profile.

The prototype was fabricated and measured in an anechoic chamber with a network analyzer Keysight E5071C. The measured and simulated S-parameter plots of the proposed antenna design are compared in Fig. 3, showing good agreement in the working band of the antenna. The measured and simulated radiation patterns at the resonant frequency of 2.45 GHz are compared

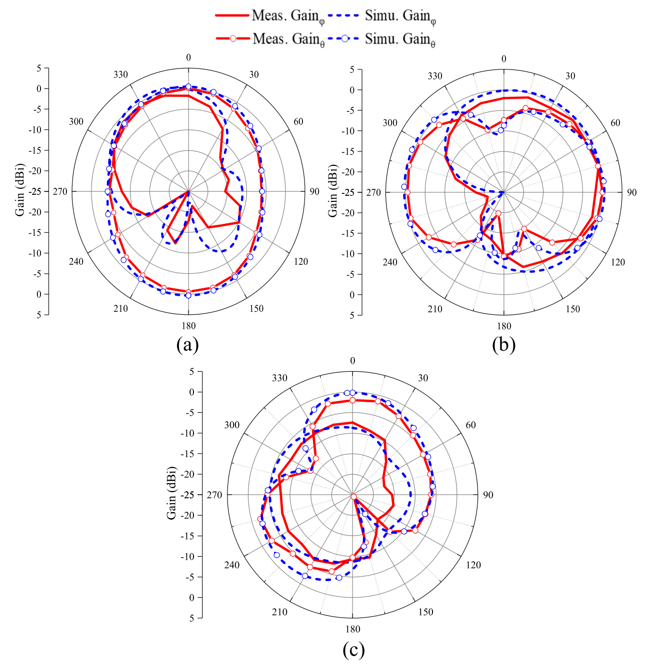

Fig. 4. Measured and simulated radiation patterns of the antenna at 2450 MHz. (a) *xy* plane. (b) *xz* plane. (c) *yz* plane.

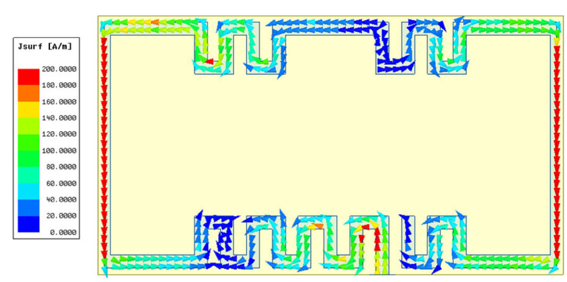

Fig. 5. Current distribution of the proposed PLMA at 2450 MHz.

in Fig. 4. It can be found that the measurement and simulation results are in good agreement. In most applications, coverage relies on the radiation pattern in the *xy* plane. In Fig. 4(a), the theta polarization (vertical) component is relatively strong with the peak theta polarization gain of 0.06 dBi, which indicates that the antenna has a good vertical radiation performance.

Fig. 5 shows the simulated surface current at 2450 MHz. It can be seen that the highest surface current densities are located in the two vertical side arms of the antenna and the current directions are the same, which meets the design target. The radiation patterns of the antenna are then dominated by the two vertical arms.

III. Comparison With Conventional Antenna Designs

In this section, the proposed planar meander line antennas are further compared with the quarter-wavelength monopole antennas in the same bands.

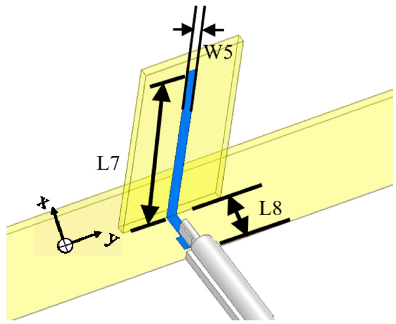

Fig. 6. Monopole antenna for comparison.

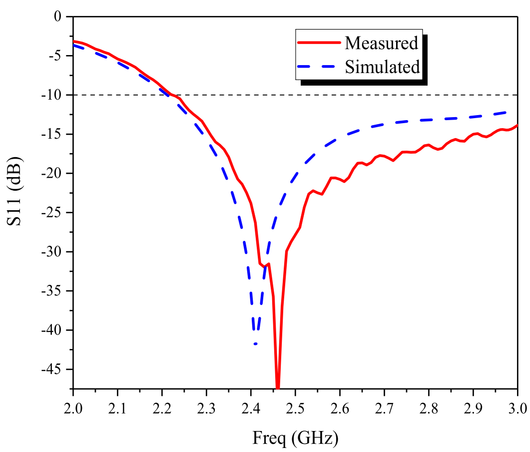

Fig. 7. Measured and simulated S-parameter plots of the monopole.

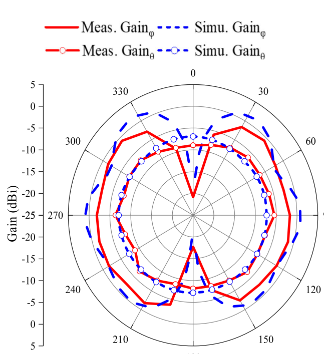

Fig. 8. Measured and simulated radiation patterns of the monopole antenna at 2450 MHz (*xy* plane).

A. Antenna Performance Comparison

A monopole antenna model used for comparison is shown in Fig. 6.

The sizes of the ground plane and the clearance are the same as the corresponding PLMA. In the figure, the monopole is shown with L7 = 18.5, L8 = 5, and W5 = 1 mm. The feeding connection for the monopole is the same as the proposed PLMA in Section II. The simulated and measured S-parameter plots of the monopole are shown in Fig. 7.

The measured and simulated radiation patterns in the *xy* plane are presented in Fig. 8. For the monopole, current flowing on the ground plane is a comparable source of radiation, thus, monopole has relatively strong horizontal (Phi) antenna gain. The measured radiation pattern results indicate that the main polarization of the monopole is horizontal, and its peak vertical (theta) polarization gain in the *xy* plane is −5.45 dBi, which is 5.51 dB less than the corresponding PLMA.

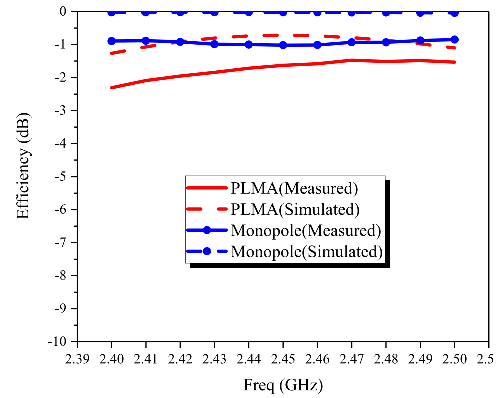

Fig. 9. Measured and simulated efficiency of PLMA and monopole.

The efficiency of the PLMA is also compared with the monopole antenna, and the results are shown in Fig. 9. In the testing process, the fabricated PLMA and monopole antennas used the same ground PCB and the same feeding cable. The proposed PLMA realizes an efficiency of −1.6 dB at 2450 MHz, whereas the efficiency of the monopole is −1 dB. The results demonstrate that the performance of the proposed PLMA design meets the requirements of the wireless router or terminal.

The simulated ground current distributions at 2.45 GHz are shown in Fig. 10, where the excitation is set as 1 W. When the monopole antenna operates, the ground plane of the PCB radiates along with the antenna. The current on the ground plane is spread out in a relatively large area. For the proposed PLMA, most of the current is concentrated on the antenna radiator itself, and the current on the ground plane is mainly distributed close to the antenna. As discussed earlier, less current distribution on the ground plane results in less dependence of the antenna performance on the close-by PCB structure, and thus potentially less RF interference.

B. Coupled Noise Measurement

As we mentioned before, the common impedance coupling could be the dominating noise coupling mechanism, therefore, RF noise is more easily coupled to internal antenna. In order to further investigate the susceptibility of the PLMA to noise, a noise coupling experiment was conducted. The configuration of the experiment is illustrated in Fig. 11.

An antenna, either a PLMA or a monopole, was placed near the 1 MΩ resistor which was fed by a 3.3 V 144 MHz clock generator. The resistor acted as a digital noise source. The antenna has the same geometry and placement as the PLMA and the monopole cases discussed in Sections II and III, respectively. The noise coupled to the antenna is directly measured by a spectrum analyzer (SA) Agilent E4404B, and the coupled noise strength is recorded 5 times in a row, the averaged value is calculated as follows. The monopole antenna and the PLMA

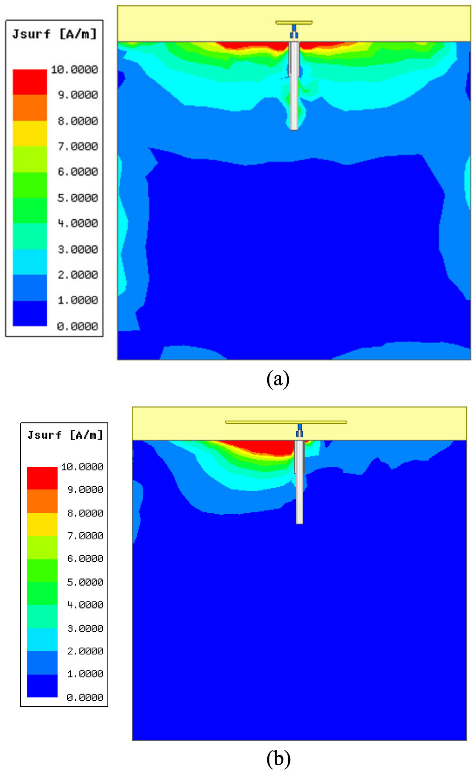

Fig. 10. Simulated current distributions at 2450 MHz of (a) monopole antenna, and (b) PLMA.

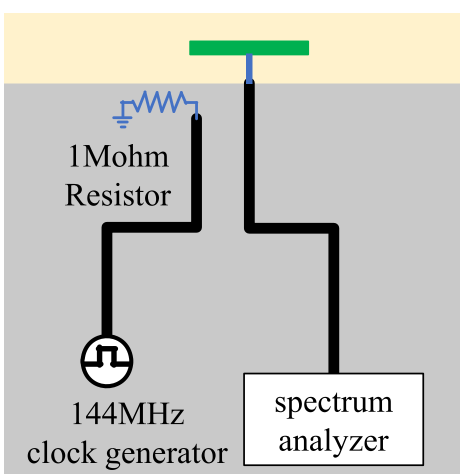

Fig. 11. Configuration of the setup for coupled noise measurement.

were placed at the same position to compare the coupled noise to the two antennas. To reduce the noise from environment, this measurement of coupled noise was conducted in an anechoic chamber. The frequency of the 17th harmonic of the digital clock is 2.448 GHz.

The measured coupled noise levels of the PLMA monopole antenna are listed in Table I. The coupled noise measurement results clearly show that the coupled noise to the PLMA is approximately 2.8 dB smaller than that to the corresponding monopole antenna.

TABLE I
COUPLED NOISE MEASUREMENT RESULTS

Antenna Type	Measured Noise Strength (dBm)					
	1	2	3	4	5	mean
Monopole	-82.67	-83.28	-82.51	-83.61	-82.85	-82.98
PLMA	-85.05	-86.32	-87.09	-84.53	-86.02	-85.80

IV. Performance Comparison in Multi-Antenna System

In a MIMO system, in order to increase receiving capability and throughput, two or more antennas working in the identical frequency bands are placed in one AP. The interaction among these antennas should be taken into consideration in antenna design. In a typical MIMO system, the efficiencies of the antennas, the balance of the antenna gains among different antennas, and the correlation among the antennas are important for the overall throughput of the receivers. Furthermore, less ground plane dependence can result in a better balance of the gains for the antennas included in the system. The ECC is an important parameter to evaluate the mutual coupling, i.e., the correlation, among antennas. In this section, the ECC between two PLMA antennas is investigated and compared with that between two monopole antennas. Furthermore, the proposed PLMA antennas were assembled on a router, and the wireless performance of the router was measured in an anechoic chamber, compared to that with two conventional monopole antennas. The over-the-air (OTA) performance of the router is an ultimate validation of the proposed antenna design.

A. ECC Comparison

ECC is an important parameter for MIMO systems. It can be calculated from the radiation patterns of the antennas, or can be simplified to (1) using the scattering parameters of the radiators in the antenna array system with good approximation [13], [14].

$$\rho_e = \frac{|S_{11}^* S_{12} + S_{21}^* S_{22}|^2}{\left(1 - |S_{11}|^2 - |S_{21}|^2\right)\left(1 - |S_{22}|^2 - |S_{12}|^2\right)}. \quad (1)$$

In the following study, all ECC values are calculated in (1).

Two identical PLMAs proposed in this article are placed in a simple two-antenna system with a PCB ground plane, and the ECC performance is compared with that of a similar system with two monopole antennas placed in the same relative locations on the same PCB ground plane.

To make meaningful comparisons, the monopole antennas are placed with the same clearance distance of 5 mm away from the PCB ground plane as the PLMAs. The geometry of the two-antenna system is shown in Fig. 12. The size of PCB is 100 mm × 150 mm, which is similar to the size of the main board of a conventional wireless router. In Fig. 12(a) and (b), the distance between the two feeding portions is D = 75 mm. The dimensions of the PLMAs and the monopoles are the same as those described in Sections II and III, respectively.

The measured and simulated S-parameter results of the two PLMAs and the two monopole antennas are plotted in Fig. 13. It can be seen that the resonant frequency of the monopole shifts to

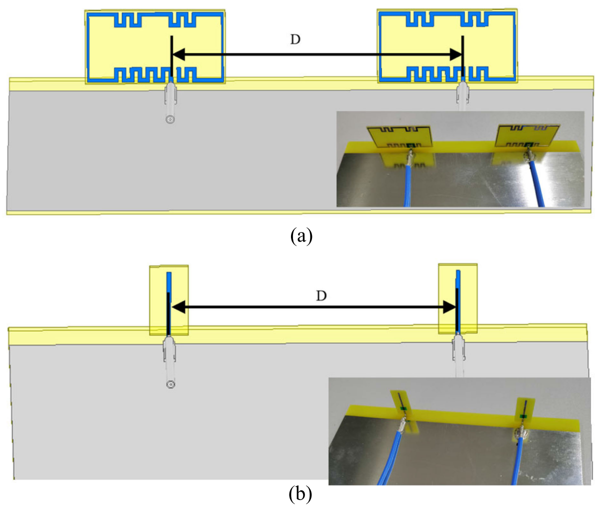

Fig. 12. Geometry of two antennas placed to a 100 mm × 150 mm main board. (a) Two identical PLMAs. (b) Two identical monopole antennas.

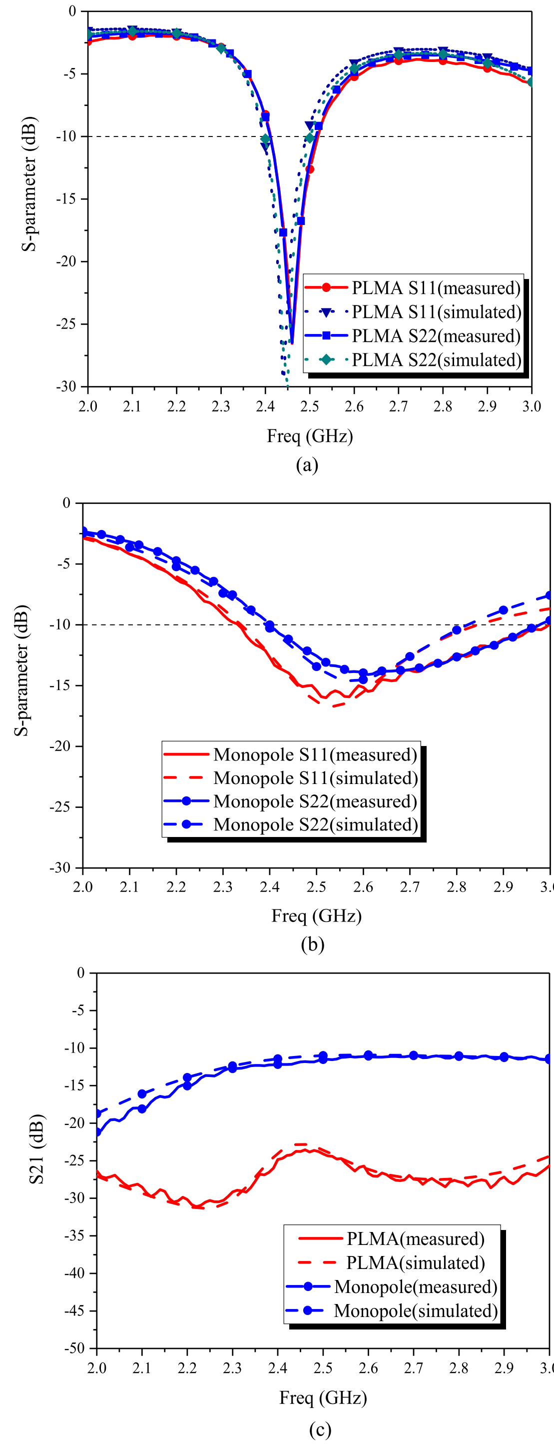

Fig. 13. Measured and simulated S-parameter results. (a) $|S_{11}|$ and $|S_{22}|$ of two PLMAs. (b) $|S_{11}|$ and $|S_{22}|$ of two monopole antennas. (c) $|S_{21}|$ of PLMAs and monopole antennas.

2.6 GHz due to the size change of the ground plane. For PLMA, its resonant frequency is nearly unchanged because of its lower dependence on the ground plane, as described in Section III.

From Fig. 13, the $|S_{11}|$ and $|S_{22}|$ results of the antennas in both the PLMA system and the monopole antenna system are acceptable in the working frequency band (2.4–2.5 GHz). The $|S_{21}|$ results, presented in Fig. 13(c), between the two PLMAs are much lower than those between the two monopole antennas in the entire frequency range. At the working frequency of 2.45 GHz, the measured $|S_{21}|$ value between the two PLMAs is –23.7 dB, approximately 11.9 dB smaller than that between the two monopole antennas, which has a value of −11.8 dB. Measured results indicate that the PLMA has better isolation with specific current distribution.

Fig. 14 shows the ECC comparisons between the PLMA system and the monopole antenna system. The measured and simulated results both validate the advantage of the proposed PLMA in a multi-antenna system. The ECC of the PLMAs is clearly lower than that of the monopole antennas from 2.4 to 2.5 GHz. This is a clear indication that, when two identical antennas are placed in a system, the correlation between the two PLMAs is significantly weaker than that between the two monopole antennas, which is desirable for MIMO performance.

Similarly analyzed as in Section III for a single antenna, the simulated current distributions of the two antenna systems on the ground plane are shown in Fig. 15, in which the left element is excited. Similar to the single antenna case, the current of the PLMAs is more concentrated near the exciting antenna, which visually explains the lower $|S_{21}|$ and the lower ECC of the system.

B. Router OTA Measurement

As mentioned earlier, less RF interference issues could be caused in the wireless terminal using the proposed antenna. Furthermore, the lower ECC could also result in a better OTA performance. To validate this idea, the proposed PLMAs were assembled on a router, and the wireless performance of the device was tested and compared to that of the same router with two corresponding monopole antennas instead. The modified device is illustrated in Fig. 16. For the selected router, the receiver is desensitized with internal antenna because of parasitic resonance. A piece of copper tape, placed upon the SoC but has no direct connection with its PCB, was used to intentionally

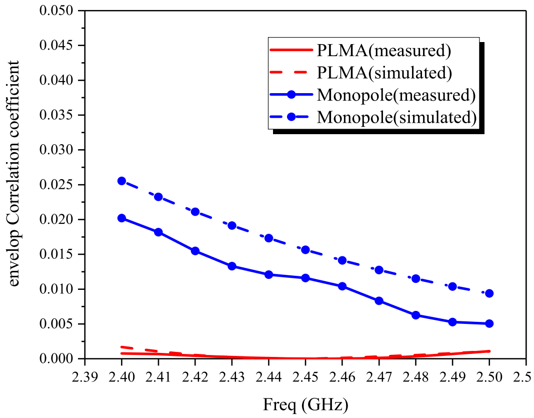

Fig. 14. Measured ECC comparison of the PLMA and monopole antenna systems.

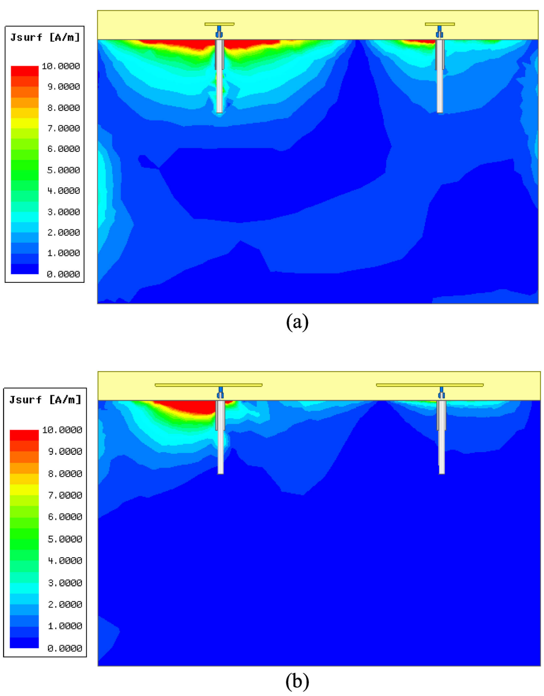

Fig. 15. Simulated current distributions of (a) two monopole antennas, and (b) two PLMAs.

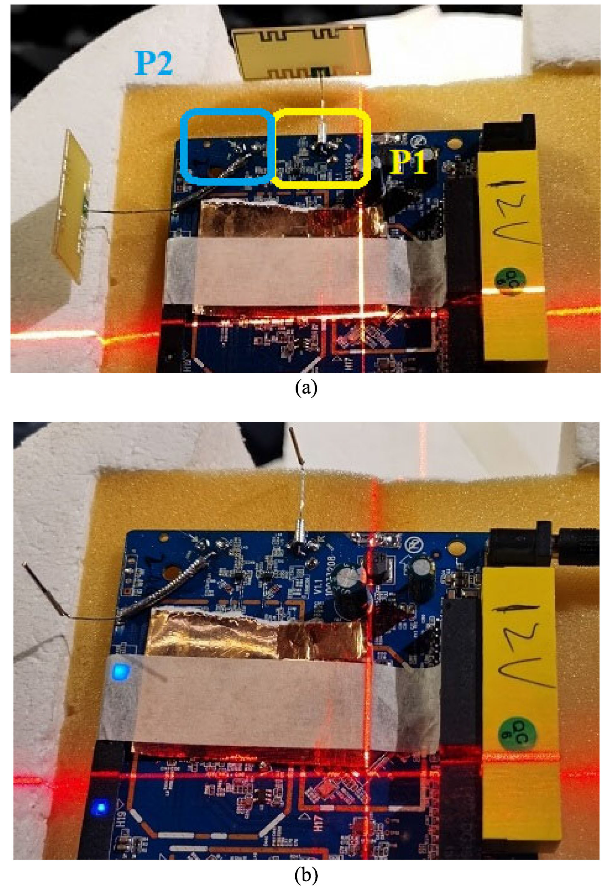

Fig. 16. Modified router assembled with (a) PLMA and (b) monopole.

TABLE II
OTA MEASUREMENT RESULTS

Antenna assembled to	TRP (dBm)		TIS (dBm)	
	PLMA	Monopole	PLMA	Monopole
Only P1	9.24	9.53	-91.51	-89.62
Only P2	10.75	11.6	-94.8	-89.06
Both P1+P2	11.53	13.39	-95.68	-90.88

enhance the interference. It should be mentioned that the feeding probe was lengthened because the resonant frequency of both PLMA and monopole shifts toward right under such placement.

The router was tested in an anechoic chamber RayZone 2800 with Rohde and Schwarz CMW500 wireless communication tester. At first, the router and CMW500 are both placed in the anechoic chamber and the conducted sensitivity on each port is measured, which the value is −95.4 dBm and −94.7 dBm, respectively. For the OTA test, the device was tested under the specifications of IEEE 802.11 g with multiple configurations, by using a constant channel no.1 (whose center frequency is 2412 MHz) and a data rate of 6 Mbps. The measured total radiated power (TRP), and total isotropic sensitivity (TIS) values are listed in Table II.

From the table, the TRP results of the PLMAs are less than the monopole antennas, which is consistent with their radiation efficiencies. The TIS values of the case with the PLMAs are lower than those with the monopole antennas under the same configuration. This indirectly validates that the PLMAs cause less RF interference and are better isolated, which are necessary to achieve better receiver sensitivity for terminal devices.

To summarize the performances between PLMA and the monopole antenna used in experiments, a comparison is listed in Table III. Overall, the currents of the proposed PLMA are concentrated on radiator itself, which results in a smaller ECC and less noise coupling. But the size of the antenna is larger than the monopole, and the efficiency is worse when the antenna was etched on a lossy substrate.

TABLE III
COMPARISON WITH MONOPOLE

features	PLMA	monopole
Size (mm)	35×19	1×18.5
Bandwidth (GHz)	5.3% (2.39 - 2.52)	31.8% (2.25 - 3.1)
Efficiency (dB) at 2.45GHz	-1.6	-1
Peak vertical polarized component (dBi) at 2.45GHz	0.06	-5.45
Measured ECC at 2.45GHz	0.000145	0.0116
Couped noise strength (dBm)	-85.8	-82.98
Measured TIS (dBm)	-95.68	-90.88

V. CONCLUSION

A full-wave wire PLMA antenna is proposed in this article for wireless terminals. Simulation and measurement have demonstrated the advantages of the antenna design.

1) The antenna is proposed with low profile.
2) Adequate vertical antenna gain and efficiency are achieved, which is appropriate for multipath indoor environment.
3) Less current distributed on the reference plane, the antenna is described and shown to have low desensitization in a noisy radio environment. Critical for designing high-sensitive routers.
4) Better isolation or ECC is achieved for MIMO applications, which results in lower correlation among multiple antennas used in a MIMO system that is also a critical factor for achieving better throughput.

The proposed PLMA is easy to fabricate with a relatively low cost. Overall, it provides a suitable antenna solution for wireless terminal devices.

REFERENCES

[1] P. Kyritsi and D. C. Cox, "Propagation characteristics of horizontally and vertically polarized electric fields in an indoor environment: Simple model and results," in *Proc. Veh. Technol. Conf.*, 2001, vol. 3, pp. 1422–1426.

[2] P. Kyritsi, D. C. Cox, R. A. Valenzuela, and P. W. Wolniansky, "Effect of antenna polarization on the capacity of a multiple element system in an indoor environment," *IEEE J. Sel. Areas Commun.*, vol. 20, no. 6, pp. 1227–1239, Aug. 2002.

[3] K.-L. Wong, H.-J. Chang, C.-Y. Wang, and S.-Y. Wang, "Very-low-profile grounded coplanar waveguide-fed dual-band WLAN slot antenna for on-body antenna application," *IEEE Trans. Antennas Propag.*, vol. 19, no. 1, pp. 213–217, Jan. 2020.

[4] K.-L. Wong and C.-Y. Tsai, "Low-profile dual-wideband inverted-T open slot antenna for the LTE/WWAN tablet computer with a metallic frame," *IEEE Trans. Antennas Propag.*, vol. 63, no. 7, pp. 2879–2886, Jul. 2015.

[5] S.-W. Su, C.-T. Lee, and S.-C. Chen, "Very-low-profile, triband, two-antenna system for WLAN notebook computers," *IEEE Trans. Antennas Propag.*, vol. 17, no. 9, pp. 1626–1629, Sep. 2018.

[6] C.-T. Lee and S.-W. Su, "Small-sized, tri-band, two-antenna system aimed for 4 × 4 Gbps notebook applications," in *Proc. Int. Symp. Antennas Propag.*, 2018, pp. 1–2.

[7] S.-G. Zhou and J.-Y. Li, "Low-profile and wideband antenna," *IEEE Antenna Wireless Propag. Lett.*, vol. 10, pp. 373–376, 2011.

[8] S. S. Alja'afreh, Y. Huang, L. Xing, Q. Xu, and X. Zhu, "A low-profile and wideband PILA-based antenna for handset diversity applications," *IEEE Antenna Wireless Propag. Lett.*, vol. 14, pp. 923–926, 2015.

[9] R.-L. Li, B. Pan, J. Laskar, and M.-M. Tentzeris, "A low-profile planar antenna for DVB-H terminals," *Microw. Opt. Technol. Lett.*, vol. 49, no. 7, pp. 1630–1633, Jul. 2006.

[10] K. V. S. Rao, P. V. Nikitin, and S. F. Lam, "Antenna design for UHF RFID tags: A review and a practical application," *IEEE Trans. Antennas Propag.*, vol. 53, no. 12, pp. 3870–3876, Dec. 2005.

[11] M. Sallam, E. Soliman, G. Vandenbosch, and W. De Raedt, "Novel electrically small meander line RFID tag antenna," *Int. J. RF Microw. Comput., Aided Eng.*, vol. 23, pp. 639–644, 2013.

[12] Y. Qi, J. Fan, Y.-H. Bi, W. Yu, and J. Drewniak, "A planar low-profile meander antenna design for wireless terminal achieving low self-interference," in *Proc. IEEE Symp. Electromagn. Compat. Signal Integrity*, 2015, pp. 320–323.

[13] S. Blanch, J. Romeu, and I. Corbella, "Exact representation of antenna system diversity performance from input parameter description," *IEEE Electron. Lett.*, vol. 39, no. 9, pp. 705–707, May 2003.

[14] C. Votis, G. Tatsis, and P. Kostarakis, "Envelope correlation parameter measurements in a MIMO antenna array configuration," *Int. J. Commun. Netw. Syst. Sci.*, vol. 3, pp. 350–354, 2010.

Yang Xiao (Student Member, IEEE) received the M.S. degree in electrical engineering from Hunan University, Changsha, China, where he is currently working toward the Ph.D. degree in electrical engineering.

His research interests include antenna design of mobile terminals, wearable antenna, and EMC issues.

Yihong Qi (Senior Member, IEEE) received the B.S. degree in electronics from the National University of Defense Technologies, Changsha, China, in 1982, the M.S. degree in electronics from the Chinese Academy of Space Technology, Beijing, China, in 1985, and the Ph.D. degree in electronics from Xidian University, Xi'an, China, in 1989.

From 1989 to 1993, he was a Postdoctoral Fellow and then an Associate Professor with Southeast University, Nanjing, China. From 1993 to 1995, he was a Postdoctoral Researcher with McMaster University, Hamilton, ON, Canada. From 1995 to 2010, he was with Research in Motion (Blackberry), Waterloo, ON, Canada, where he was the Director of advanced electromagnetic research. He is currently a Scientist with Peng Cheng Laboratory, Shenzhen, China. He is also the President and the Chief Scientist with General Test Systems, Inc., Shenzhen, China. He founded DBJay (DBJ Technologies), Zhuhai, Guangdong, China, in 2011. He is also an Adjunct Professor with the Electromagnetic Compatibility Laboratory, Missouri University of Science and Technology, Rolla, MO, USA, an Adjunct Professor with Western University, London, Ontario, Canada, Honorary Professor with Southwest Jiaotong University, Chengdu, and an Adjunct Professor with Hunan University, Changsha, China. He holds more than 500 published and pending patents.

Dr. Qi received the 2017 Technology Achievement Award from the IEEE EMC Society. He was a Distinguished Lecturer of the IEEE EMC Society from 2014 to 2015, and the founding Chairman of the IEEE EMC TC-12. He is a Fellow of the Canadian Academy of Engineering and the National Academy of Inventors.

Wei Yu (Member, IEEE) received the B.S. degree in electrical engineering from Xi'an Jiaotong University, Xi'an, China, in 1991, the M.S. degree in electrical engineering from the China Academy of Space Technology, Beijing, China, in 1994, and the Ph.D. degree in electrical engineering from Xidian University, Xi'an, China, in 2000.

From 2001 to 2003, he was a Postdoctoral Fellow with the University of Waterloo, Waterloo, ON, Canada. From 2008 to 2012, he was a CTO with Sunway Communications, Ltd. He founded Antennovation Electronics, Inc., in 2004 and cofounded General Test Systems, Inc., Shenzhen, China, in 2012. He is currently with DBJ Technologies, Zhuhai, China, as a COO. His current research interests include signal processing and mobile device test system. He is an inventor of 32 published and pending patents.

Ye-Hai Bi was born in Shanghai, China. He received the B.S. degree in electronic information science and technology, and the M.S. degree in radio physics from the University of Electronic Science and Technology of China, Chengdu, China, in 2003 and 2006, respectively.

In April 2006, he joined Shanghai Amphenol Airwave as an RF Antenna Engineer and then as a Senior Design Engineer. He is involved in several mobile terminal antenna design projects for international and domestic customers, such as Motorola, Sony Ericsson, and Huawei. Since May 2010, he has been an RF Manager with Shenzhen Sunway Communication Company, Ltd., Shanghai branch, China. His research interests include compact size, wideband antennas for 3G/LTE mobile devices, and smart antennas for wireless AP/ router.

Xiangrui Su (Student Member, IEEE) received the B.S. degree in electrical engineering from Zhejiang University, Hangzhou, China, in June 2019. He is currently working toward the Ph.D. degree in electrical engineering with EMC Lab of Missouri University of Science and Technology, Rolla, MO, USA, from 2019 to 2024.

He was a student intern with Apple. His research interests include RFI source reconstruction and coupling paths analysis, and the conductive emission modeling based on hybrid simulation.

Chunyu Wu received the bachelor's degree in electrical engineering from Huazhong University of Science and Technology, Wuhan, China, in 2014, and the M.S. and Ph.D. degrees in electrical engineering from Missouri University of Science and Technology, Missouri, MO, USA, in 2017 and 2020, respectively.

His research interests include signal integrity, power integrity, and EMC.

Qiang Liu (Member, IEEE) received the B.S. degree in applied physics from the Hunan University of Science and Technology (HUST), Xiangtan, China, in 2004, the M.S. degree in electronic engineering from the National University of Defense and Technology, Changsha, China, in 2007, and the Ph.D. degree in electronic engineering from the Beijing University of Posts and Telecommunications, Beijing, China, in 2014.

From March 2007 to August 2011, he was a Lecturer with the School of Physics and Electronics, HUST. In 2014, he joined the College of Electrical and Information Engineering, Hunan University, Changsha, China, where he is currently an Associate Professor. From 2016 to 2017, he was a Visiting Research Fellow with RF and Microwave Laboratory, National University of Singapore. His current research interests include microwave components and antennas.

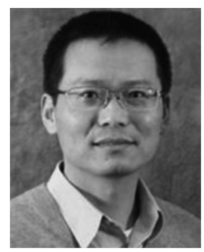

Jun Fan (Fellow, IEEE) received the B.S. and M.S. degrees from Tsinghua University, Beijing, China, in 1994 and 1997, respectively, and the Ph.D. degree from Missouri S&T, Rolla, MO, USA, in 2000, all in electrical engineering.

From 2000 to 2007, he was a Consultant Engineer with NCR Corporation, San Diego, CA, USA. In July 2007, he joined Missouri S&T, where he was a Professor and a Director of the EMC laboratory. He also served as the Director of the National Science Foundation Industry/University Cooperative Research Center for Electromagnetic Compatibility and as a Senior Investigator with the Missouri S&T Material Research Center. He is currently an Adjunct Professor with Missouri S&T. His research interests include signal integrity and EMI design in high-speed digital systems, dc power-bus modeling, intrasystem EMI and RFI, PCB noise reduction, differential signaling, and cable/connector designs.

Dr. Fan was the recipient of the IEEE EMC Society Technical Achievement Award in August 2009. He is currently an Associate Editor for IEEE TRANSACTIONS ON ELECTROMAGNETIC COMPATIBILITY and *IEEE EMC Magazine*.